Density-functional-based tight-binding calculation of excitons in conjugated polymers

Thomas G. Pedersen
Aalborg University, Institute of Physics, Pontoppidanstræde 103, DK-9220 Aalborg Øst, Denmark
(Received 3 April 2003; revised manuscript received 14 October 2003; published 19 February 2004)

The fundamental excitations and optical properties of four important conjugated polymers (*trans*-polyacetylene, polydiacetylene, poly-*para*-phenylene, and polyphenylenevinylene) are described within a method combining density-functional-based tight-binding and the Bethe–Salpeter equation. This non-self-consistent approach is computationally highly efficient and can potentially be applied to very complex structures. We find that both singlet and triplet excitons generally agree with measurements. Moreover, the calculated UV/visible optical spectra reliably reproduce location and polarization of most experimental resonances.

DOI: 10.1103/PhysRevB.69.075207 PACS number(s): 78.40.Me, 78.20.Bh, 71.35.Cc

I. INTRODUCTION

The calculation of excitons in inorganic or organic semiconductors is a requirement for a full understanding of the optical properties of these materials. For bulk and low-dimensional inorganic semiconductors the effective mass description of Wannier excitons has been applied for many years. There is, however, a growing consensus that more refined methods such as the Bethe–Salpeter approach are needed for accurate results.[1–3] A prominent example is the case of indirect band gap materials such as Si, for which excellent agreement with experimental spectra has been demonstrated.[1,3] However, even for direct band gap materials there is a clear need for accurate methods if the optical properties above the vicinity of the band gap are considered.

For conjugated polymers and other quasi-one-dimensional materials a similar situation is encountered. The long-axis optical response in the vicinity of the band gap can be described within the effective mass picture.[4–6] However, higher resonances and, in particular, excitations perpendicular to the polymer axis depend intimately on the detailed band structure and chemical structure that are ignored in the effective mass approximation. Several convincing applications of the Bethe–Salpeter approach to conjugated polymers have been published.[7–9] Unfortunately, the full density-functional theory + Bethe–Salpeter approach is rather computationally demanding. This ultimately limits the applicability to structures with small unit cells and excludes structures like chiral carbon nanotubes, which represent highly exciting challenges. For this reason, we have recently[10] explored the much less demanding density-functional-based tight-binding (DF-TB) method[11] and applied it to exciton optical and electro-optic properties of poly-*para*-phenylene and polyphenylenevinylene. The reasonable results obtained for binding energies of the lowest singlet exciton are encouraging indications of the accuracy of the DF-TB method.

The purpose of this paper is to present a much more detailed study of the combined DF-TB + Bethe–Salpeter method applied to excitonic optical properties of conjugated polymers. Hence, we include (1) calculation of the relaxed geometry, (2) both singlet and triplet excitons, (3) long- as well as short-axis UV/visible optical spectra for four important materials: *trans*-polyacetylene (PA), polydiacetylene (PDA), poly-*para*-phenylene (PPP), and polyphenylenevinylene (PPV). In particular, results for higher resonances in the optical response are presented. We find that exciton effects lead to a complete rearrangement of the optical spectra for both long- and short-axis components. Our findings are compared to experimental spectra for highly oriented *trans*-polyacetylene,[12] crystalline bis(*p*-toluene sulfonate) polydiacetylene,[13] thin-film ladder-type poly-*para*-phenylene,[14] and oriented poly[(2-methoxy, 5-(2′-ethyl)-hexyloxy) *para*-phenylene vinylene].[15] In all these polymers, the π-conjugated backbones are essentially planar provided defect density is low. Hence, even though we replace side-group and substituents by hydrogens in the calculations, we restrict all conformations to planar ones. In general, calculated singlet as well as triplet excitons are in good agreement with experiments including higher singlet excitons detected in the UV/optical response. Taken together, we find that the DF-TB + Bethe–Salpeter approach provides an accurate and computationally efficient description of excitonic properties in conjugated polymers.

II. THEORETICAL FRAMEWORK

The DF-TB method was originally developed for hydrocarbons[11] but has since been applied to a range of materials including silicon,[16] complex organic molecules,[17] various nanotube structures,[18,19] and also metal-semiconductor contacts.[20] Its great simplicity lies in the fact that all two-center integrals as well as the repulsive two-body potentials are parametrized functions of distance. These functions are obtained from density-functional theory (DFT) in the local density approximation for isolated atoms and diatomic molecules using a ''compression'' potential to mimic the influence of surroundings.[11] A ''self-consistent charge'' extension has been formulated[17] but the original method is not self-consistent and all iteration steps are avoided. Nevertheless, the method reproduces structures and vibrational frequencies with remarkable accuracy. In the case of planar conjugated molecules, the method has the additional advantage that π and σ electrons are completely decoupled. In ordinary DFT this is not the case since orbitals of different symmetry are coupled via the contributions to the electron density. In the present case, we only consider planar conformations and, thus, π–σ decoupling allows us to ignore the σ-electron bands that are of relatively little importance

for the optical properties in the UV/visible spectral range.

In our previous work[10] dealing with the high-field electro-optic response, we treated conjugated polymers as large but finite molecules comprised of 30 to 40 monomers. This approach was partly dictated by the need of including an external electrostatic potential that breaks the translational symmetry and makes it impossible to apply periodic boundary conditions. In the present work, we focus on intrinsic optical properties and exclude external fields. Thus, periodic boundaries are assumed throughout, which corresponds to considering a ring rather than a linear chain of monomers. This approach is similar to that applied by Abe and co-workers.[21,22] In this manner, Bloch sums formed from the αth π-orbital within the monomer or unit cell can be written as

$$\chi_{\alpha k}(\mathbf{r}) = \frac{1}{\sqrt{N}} \sum_{n=1}^{N} e^{ikna} \phi(\mathbf{r} - \mathbf{r}_{\alpha n}), \tag{1}$$

where a is the lattice constant, N is the number of unit cells in the ring, $k = \pi(2p - N - 2)/(aN)$ with $p = 1,2,...N$, is the wave number, and $\phi(\mathbf{r} - \mathbf{r}_{\alpha n})$ is a localized π-orbital centered at the αth position of the nth unit cell. The matrix elements between such Bloch sums are calculated using the DF-TB framework and leads to a simple generalized eigenvalue problem.

Once the band states $\varphi_{ik}(\mathbf{r})$ are obtained as linear combinations of Bloch sums, i.e., $\varphi_{ik}(\mathbf{r}) = \Sigma_\alpha c_{\alpha k}^{(i)} \chi_{\alpha k}(\mathbf{r})$, the Bethe–Salpeter equation for the exciton states can be set up. The exciton states are expanded in valence ($i = v$) and conduction ($i = c$) band states as $\psi_{\text{exc}}(\mathbf{r},\mathbf{r}') = \Sigma_{kvc} A_{kvc} \varphi_{ck}(\mathbf{r}) \varphi_{vk}^*(\mathbf{r}')$. The matrix problem constructed for the expansion coefficients A_{kvc} and exciton energy eigenvalue E_{exc} reads as[2,3,7–9]

$$\sum_{k'v'c'} [2V^x_{kvc,k'v'c'} \delta_{S,0} - W_{kvc,k'v'c'}] A_{k'v'c'} = [E_{\text{exc}} - E_{ck} + E_{vk}] A_{kvc}. \tag{2}$$

Here, E_{ck} and E_{vk} are conduction and valence band eigenvalues, respectively. Electrons and holes are coupled via the Coulomb matrix element $W_{kvc,k'v'c'}$ and the exchange matrix element $V^x_{kvc,k'v'c'}$. The factor $\delta_{S,0}$ implies that the exchange interaction is present for singlet excitons with vanishing total spin S only. When the bands states are expanded in Bloch sums and Eq. (1) is used, the exciton matrix elements are ultimately expressed in terms of Coulomb and exchange integrals between localized π orbitals. Among these four-center terms only a small fraction are of importance due to the exceedingly small overlap between distant π orbitals. Hence, terms with more than two different sites involved are discarded. The question of screening is temporarily left aside and we consider the following bare Coulomb and exchange integrals:

$$(0,n|n,0) = \int\int \frac{|\phi(\mathbf{r})|^2 |\phi(\mathbf{r}' - \mathbf{r}_n)|^2}{|\mathbf{r} - \mathbf{r}'|} d^3r d^3r', \tag{3}$$

and

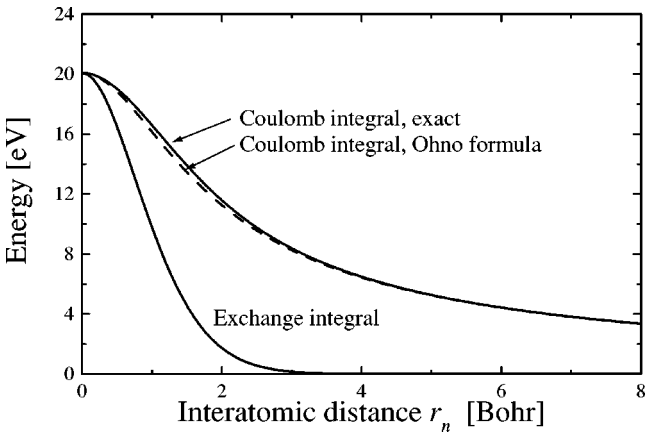

FIG. 1. Calculated Coulomb and exchange integrals vs interatomic distance. The dashed line is an Ohno-type fit to the exact curve.

$$(0,n|0,n) = \int\int \frac{\phi(\mathbf{r})\phi^*(\mathbf{r} - \mathbf{r}_n')\phi^*(\mathbf{r})\phi(\mathbf{r}' - \mathbf{r}_n)}{|\mathbf{r} - \mathbf{r}'|} d^3r d^3r'. \tag{4}$$

As the spatial behavior of the π orbitals is known explicitly in DF-TB (in contrast to empirical tight-binding) these integrals can be evaluated. The results are plotted in Fig. 1 together with an Ohno-type approximation $(0,n|n,0) \approx \omega_0 (1 + \omega_0^2 r_n^2)^{-1/2}$ with $\omega_0 = 20.08$ eV for the Coulomb integral. The fit is seen to be quite satisfactory. The Coulomb integral decays asymptotically as $1/r_n$ whereas the exchange integral has a rapid exponential decrease. In fact, the exchange integral is closely approximated by an on-site interaction since the value at a typical interatomic distance of 2.6 bohr is only approximately 2% of the on-site value $(0,0|0,0)$. We consequently ignore all non-on-site exchange integrals, i.e., terms like $(0,n|0,n)$ are neglected whenever $n \neq 0$. Hence, with this step, all integrals over atomic orbitals of the same argument but located on different sites are ignored. It is noted that this also goes for the X-term $(0,0|0,1) = (0,0|1,0)$ that has been considered in previous models.[23] This term, however, also decays exponentially with distance and at 2.6 bohr we find that it amounts to only 12% of the on-site integral. This finally allows us to express the Coulomb and exchange matrix elements as

$$W_{kvc,k'v'c'} = \frac{1}{N} \sum_{\alpha,\beta} c_{\alpha k}^{(v)*} c_{\alpha k'}^{(v')} c_{\beta k}^{(c)} c_{\beta k'}^{(c')*} \sum_{n=1}^{N} e^{i(k'-k)na} \times (0\alpha, n\beta|n\beta, 0\alpha)_W, \tag{5}$$

and

$$V^x_{kvc,k'v'c'} = \frac{1}{N} \sum_{\alpha,\beta} c_{\alpha k}^{(v)*} c_{\beta k'}^{(v')} c_{\alpha k}^{(c)} c_{\beta k'}^{(c')*} \times \sum_{n=1}^{N} (0\alpha, n\beta|n\beta, 0\alpha)_V, \tag{6}$$

where subscripts W and V indicate that different implementations of screening are needed for the two types of interac-

tions. In the double-index notation (such as $n\beta$) used in the four-center integrals, the first and second indices refer to unit cell and relative position within a unit cell, respectively.

The question of screening is a delicate one. As pointed out by van der Horst *et al.*[8,24] the anisotropy of polymer chains has important consequences for the screened interaction. If the symmetry of the one-dimensional system is approximately uniaxial (cylindrical) with x along the polymer long axis, then the dielectric tensor reads as $\vec{\varepsilon}=\mathrm{diag}(\varepsilon_x,\varepsilon_y,\varepsilon_y)$ and the screened Coulomb interaction between oppositely charged point charges is[25]

$$V(x,y,z)=-\frac{1}{\sqrt{\varepsilon_y^2x^2+\varepsilon_x\varepsilon_y y^2+\varepsilon_x\varepsilon_y z^2}}. \tag{7}$$

For this reason we have approximated the screened Coulomb integral by the following screened Ohno-type expression:

$$(0,n|n,0)_W\approx\frac{\omega_0}{\sqrt{\varepsilon_x\varepsilon_y+\omega_0^2(\varepsilon_y^2x_n^2+\varepsilon_x\varepsilon_y y_n^2)}}. \tag{8}$$

Next, we need to consider whether the exchange interaction should be screened or not. From many-body perturbation theory it is well established that if all quasiparticle corrections are included in a full set of single-particle excitations and all charges are taken into account in the quasiparticle calculation the exchange interaction should be via the *bare* Coulomb potential.[2–3,7–9] On the other hand, if a molecule is treated as embedded in a surrounding medium whose only influence is via screening the situation is less clear. In many semi-empirical studies based on Pariser–Parr–Pople parametrization such as Refs. 21 and 22, the exchange interaction is taken as fully screened. The tacit justification for this approach is that electronic states are calculated for individual polymer chains with no coupling to other chains. Moreover, it has been rigorously shown that the exchange interaction must be screened if only a *finite* set of single-particle excitations is taken into account.[26] In the present work, we have taken a rather pragmatic approach based on the following premises. First, the large long-axis dielectric constant ε_x is almost entirely due to self-screening within a single polymer chain. Hence, this contribution must be excluded from the exchange interaction. Second, the screening due to charges on surrounding polymer chains should be included in the exchange interaction to a certain extent. This leads us to consider the following form:

$$(0,n|n,0)_V\approx\frac{\omega_0}{\varepsilon_{\mathrm{exc}}\sqrt{1+\omega_0^2(x_n^2+y_n^2)}}. \tag{9}$$

The values adopted for the dielectric constants are discussed in the following. The parametrizations Eqs. (8) and (9) allow us to calculate numerically the exciton matrix with relatively small computational effort.

III. IMPLEMENTATION

The starting point for the implementation is a geometry optimization using the parametrized DF-TB repulsive two-body potentials. To this end we obviously need to include σ as well as π electrons. All geometric parameters including C-H distances and C-C-H angles are allowed to relax within the (x,y) plane. The lattice constants obtained in this manner are: 2.46 Å (PA), 4.93 Å (PDA), 4.28 Å (PPP), and 6.49 Å (PPV). The relaxed geometries are available from the author on request. When the band gap is calculated for the relaxed structures we generally find that it is unrealistically small. This ''band gap problem'' is a common weakness of most density-functional-based approaches. We correct the band gap by rigidly shifting the conduction bands upwards using the ''scissors operator,'' which can be regarded as a simplistic implementation of quasiparticle corrections.[8] The shifts applied for this purpose are 1.47 eV (PA), 0.79 eV (PDA), 0.97 eV (PPP), and 1.20 eV (PPV). They have been adjusted so that the lowest singlet exciton coincides with the fundamental absorption peaks measured in Refs. 12–15. It should be noted, however, that the calculated exciton binding energies defined as the difference between band gap and exciton energy are independent of the scissors operator shifts.

For the short-axis element of the dielectric tensor we have taken $\varepsilon_y=3$, which has been proved to be an appropriate value for conjugated polymers.[8] The long-axis element ε_x can be taken directly from experiments. However, different experiments yield somewhat inconsistent values. Taking *trans*-polyacetylene as one of the best-studied materials, ε_x varies from $\varepsilon_x=2.52^2\approx6.4$[27] measured at 0.62 eV to $\varepsilon_x\approx10.5$.[12] We have found that an intermediate value of $\varepsilon_x=7$ is a reasonable compromise and this value has been used for all materials. As argued earlier, the short-axis screening should be partially included in the exchange interaction and for this part we have taken $\varepsilon_{\mathrm{exc}}=2$. The sensitivity to the value of these parameters is discussed in the subsequent section. The number of π-orbital bands in the four polymers are 2 (PA), 4 (PDA), 6 (PPP), and 8 (PPV). However, for the optical properties in the UV/visible range the most remote of these bands are of little importance and, hence, we have neglected the two most remote bands of PPP and PPV in the calculation of exciton states. In addition, the number of unit cells is taken as 200 (PA), 100 (PDA), 100 (PPP), and 70 (PPV). Hence, the dimension of the exciton matrix is 400 (PA, PDA, and PPP) and 630 (PPV), which is easily handled numerically. As in our previous work,[10] we apply a recursive Green's function technique[2] to calculate the dielectric function $\varepsilon(\omega)=\varepsilon_R(\omega)+i\varepsilon_I(\omega)$ given by

$$\varepsilon(\omega)=1+\frac{2e^2}{\varepsilon_0 lA}\sum_{\mathrm{exc}}\frac{|\langle\mathrm{exc}|\mathbf{r}\cdot\hat{n}|0\rangle|^2}{E_{\mathrm{exc}}-\hbar\omega-i\hbar\Gamma}, \tag{10}$$

where $l=Na$ is the length of a polymer chain, A is the cross-sectional area of a chain taken as 20 Å^2, $\hbar\Gamma$ is a phenomenological damping constant taken as $\hbar\Gamma=0.15$ eV, and $\hat{n}$ is the unit vector of the optical electric field so that $\mathbf{r}\cdot\hat{n}=x$ and $\mathbf{r}\cdot\hat{n}=y$ for long- and short-axis properties, respectively. Using the commutation relation $\mathbf{p}=im/\hbar[H,\mathbf{r}]$ between momentum $\mathbf{p}$, Hamiltonian H, and position $\mathbf{r}$ we obtain for the dipole moments

TABLE I. Calculated band gaps (including scissors shift) and exciton energies for different conjugated polymers.

Polymer	Band gap (eV)	Low. singlet exciton (eV)	Low. triplet exciton (eV)
PA	2.07	1.70	1.25
PDA	2.56	2.00	1.37
PPP	3.40	2.72	2.22
PPV	3.01	2.40	1.86

$$\langle \mathrm{exc}|\mathbf{r}\cdot\hat{n}|0\rangle = \frac{\hbar}{im}\sum_{kvc} A_{kvc}\frac{\langle \varphi_{vk}(\mathbf{r})|\mathbf{p}\cdot\hat{n}|\varphi_{ck}(\mathbf{r})\rangle}{E_{ck}-E_{vk}}, \quad (11)$$

where, in turn, the band-to-band momentum matrix element $\langle \varphi_{vk}(\mathbf{r})|\mathbf{p}\cdot\hat{n}|\varphi_{ck}(\mathbf{r})\rangle$ is expressed in terms of momentum matrix elements between Bloch sums given by[28]

$$\langle \chi_{\alpha k}(\mathbf{r})|\mathbf{p}\cdot\hat{n}|\chi_{\beta k}(\mathbf{r})\rangle = \frac{im}{\hbar}\hat{n}\cdot\sum_{n=-1,0,1} e^{ikna}(\mathbf{r}_{0\alpha}-\mathbf{r}_{n\beta}) \times\langle \phi(\mathbf{r}-\mathbf{r}_{0\alpha})|H|\phi(\mathbf{r}-\mathbf{r}_{n\beta})\rangle. \quad (12)$$

Due to the rapid decay of orbital overlap with distance, the summation above need only cover the central unit cell and its nearest neighbors. It is noted that no intra-atomic contributions appear as only p_z-type atomic orbitals are considered.

IV. RESULTS AND DISCUSSION

Before addressing the optical spectra we consider the fundamental excitations. For the four different polymers the results are summarized in Table I. The band gaps listed include the scissors operator shifts. As mentioned above, the gap is adjusted to bring the lowest singlet exciton (shown as the second column) into agreement with experiments. The final column lists the position of the lowest triplet exciton. The triplet energies are between 53% and 65% of the band gap, which attests to the large exciton effect in conjugated polymers. The calculated singlet binding energies vary between 0.37 and 0.68 eV, which is more than an order of magnitude larger than the values observed in bulk inorganic semiconductors. In order to directly compare with experiments, we have compiled a list of singlet and triplet exciton *binding* energies in Table II. Note that in the cases of PPP and PPV the triplet binding energies are obtained from experimental singlet binding energies by adding experimental singlet–triplet splittings of 0.62 eV[34] and 1.0 eV,[35] respectively. The calculated binding energies are in reasonable agreement with experiments where available. The largest errors are around 25%, which must partially be attributed to our simple chemical structures ignoring side-groups. In addition, different experimental methods are known to produce somewhat different values for the binding energies. Hence, the overall agreement is rather convincing.

The simplistic implementation of screening in the present approach is a potential source of error. Naturally, a self-consistent implementation would lead to higher reliability.

TABLE II. Comparison of theoretical and experimental binding energies for both singlet and triplet excitons.

Polymer	Singlet exciton binding energy (eV)	Triplet exciton binding energy (eV)
PA (theory)	0.37	0.84
PA (expt.)[a]	0.50	⋯
PDA (theory)	0.56	1.19
PDA (expt.)[b]	0.57–0.59	1.40
PPP (theory)	0.68	1.18
PPP (expt.)[c]	0.50–0.85	1.12–1.47
PPV (theory)	0.61	1.15
PPV (expt.)[a,d]	0.20–0.60	1.20–1.60

[a]Reference 29.
[b]References 30 and 31.
[c]References 32–34.
[d]References 35 and 36.

However, such an extension would not be possible without abandoning the computational simplicity that is a central part of the approach. Fortunately, van der Horst and co-workers[8,24] have demonstrated from their comparison with *ab initio* calculations that the approximation $\varepsilon_y = 3$ for the important transverse dielectric constant is, in fact, not too severe. The influence of the remaining dielectric constants ε_x and $\varepsilon_{\mathrm{exc}}$ used in the present work can be judged from their influence on the exciton binding energies. Taking PA as an example, the results in Table III can be used to estimate the sensitivity to these parameters. The first row shows the results using $\varepsilon_x = 7$ and $\varepsilon_{\mathrm{exc}} = 2$ as above and the remaining rows are the results of varying the parameters around these values. It is noted that the variations for singlets and triplet are at most 0.04 and 0.06 eV, respectively. In addition, only triplets do not feel the exchange interaction and, hence, do not depend on $\varepsilon_{\mathrm{exc}}$ at all. Thus, based on these observations we judge that excitonic effects are not critically sensitive to the precise values of these parameters. On the other hand, it is clear that all results will be extremely sensitive to any variation in ε_y. The transverse screening, however, is largely determined by the surroundings of the polymer chain (e.g., solvent or other chains)[24] and these additional interactions are excluded from the present model anyway. The value $\varepsilon_y = 3$ is the appropriate one for chains in polymer films. Hence, to simulate isolated chains or chains in various solvents other values of ε_y must be used. In the discussion of

TABLE III. Exciton binding energies of *trans*-polyacetylene calculated for the lowest singlet and triplet using $\varepsilon_y = 3$ but different values for ε_x and $\varepsilon_{\mathrm{exc}}$.

ε_y	ε_x	$\varepsilon_{\mathrm{exc}}$	Singlet exciton (eV)	Triplet exciton (eV)
3	7	2	0.37	0.82
3	7	1.5	0.33	0.82
3	7	2.5	0.41	0.82
3	6	2	0.39	0.88
3	8	2	0.36	0.78

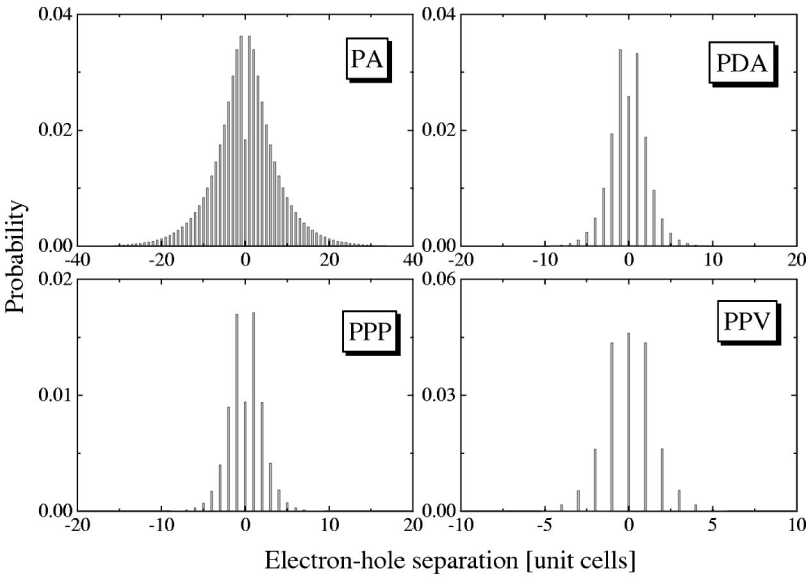

FIG. 2. Histograms for the probability of locating an electron in a particular unit cell with the hole fixed at the zeroth cell. The location of both electrons and holes is taken as the central atom in the unit cell.

PPV to follow, the dependence of exciton binding energies on ε_y is examined in more detail.

Apart from experimental data, it is quite instructive to compare the present results to more sophisticated calculations based on full DFT and empirical screening as in Ref. 8 and full DFT combined with self-consistent screening as in Ref. 7. Specifically, we focus on the binding energy of the lowest singlet exciton in PA and PPV since these materials are considered in both Refs. 7 and 8, as well as in the present work. The values obtained are 0.4 eV (PA) and 0.9 eV (PPV) in Ref. 7 and 0.43 eV (PA) and 0.54 eV (PPV) in Ref. 8. These numbers should be compared to the values 0.37 eV (PA) and 0.61 eV (PPV) obtained above. Hence, our values are quite close to those of Ref. 8, as expected from the similarities between the two approaches. In contrast, the binding energy of 0.9 eV obtained for PPV in Ref. 7 is much greater than our value as well as that of Ref. 8. At first sight, this might indicate that self-consistent screening is essential in this case. However, as clearly demonstrated in Ref. 24, the reason for the discrepancy is that *isolated* chains were considered in Ref. 7. In contrast, the transverse screening $\varepsilon_y = 3$ applied here and in Ref. 8 is appropriate for chains screened by molecules in their surroundings. Hence, our approach applies to polymers in, e.g., dense films and the agreement with Ref. 8 and experimental data are indications that reliable predictions are obtained in this case. The pronounced dependence of binding energies on ε_y is clearly seen in the calculated optical spectra of PPV that are presented at the end of this section.

The spatial localization of excitons is a manifestation of the large Coulomb forces in conjugated polymers. Depending on whether excitons extend over many unit cells or essentially a single unit cell they are classified, respectively, as Wannier or Frenkel excitons. To address this question we have illustrated in Fig. 2 the probability of finding an electron in a particular unit cell given that the hole is located in the zeroth cell. The electrons and holes have been placed on the atom nearest the center of their respective unit cells shown as insets in Figs. 3–6. In the case of PA, PDA, and PPP, the left-most among the equivalent central atoms has been used. The figure shows the probability distributions for the lowest singlet excitons obtained in this manner. It is seen that the spread ranges from many unit cells in the case of PA to very few in the case of PPV. It should be kept in mind, however, that the size of the unit cell varies greatly among the different materials. A more direct measure of the localization is the full width at half maximum for which we find the following values 30 Å (PA), 21 Å (PDA), 18Å (PPP), and 19 Å (PPV). It is noticed that the PA width is much larger than the others, in agreement with the somewhat lower binding energy obtained for this material (Table II.). Also, it is seen that while the exciton in PA may reasonably be char-

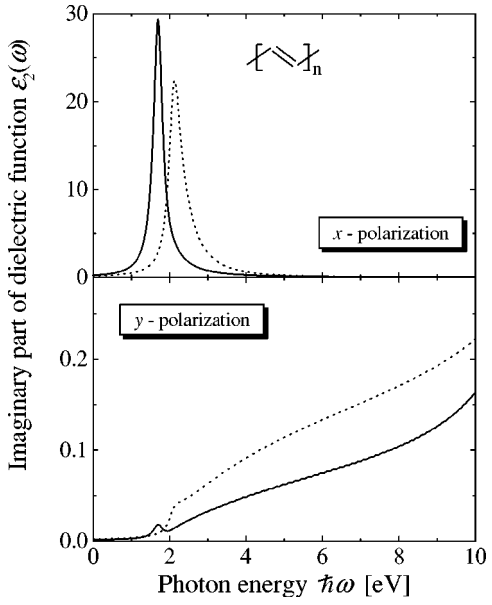

FIG. 3. Theoretical absorption spectra for *trans*-polyacetylene (PA). Full and dashed lines show calculations with and without exciton effects, respectively. The upper panel is for light polarized along the polymer long-axis and the lower panel is for the short-axis within the molecular plane.

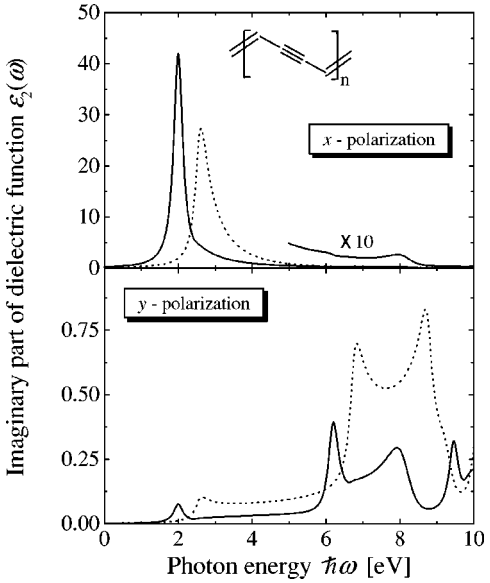

FIG. 4. Theoretical absorption spectra for polydiacetylene (PDA) using the same format as in Fig. 3. Notice the weak feature around 8 eV in the long-axis exciton spectrum.

acterized as a Wannier exciton, the other cases actually lie in between the Frenkel and Wannier limits. Finally, it is noted that the widths found for PA and PPV are roughly the same as those obtained in Ref. 7 (judged to be approximately 13 and 5 unit cells, respectively) using full DFT and self-consistent screening. This indicates that also wave functions are reliably reproduced by the present method.

Next, we turn to the optical spectra obtained from the calculated singlet excitons. In Figs. 3–6 the theoretical spectra for the imaginary part of the dielectric constant $\varepsilon_I(\omega)$ using both polarizations are shown. Full and dotted curves represent results with and without exciton effects, respectively. Where necessary, we have expanded portions of the curves in order to display low-intensity resonances more clearly. Starting with PA in Fig. 3, it is seen that in the long-axis case (x-polarization) exciton effects simply shift the fundamental resonance to lower energies and leads to a more symmetric peak. The fact that the position of the single peak of PA coincides with the experimental spectra[12] is not surprising as this is precisely the requirement used to determine the scissors operator shift. For the perpendicular polarization, the spectrum is also redshifted and a small peak is visible at the position of the fundamental singlet exciton. Compared to the long-axis spectrum, though, the intensity of the y-polarization spectrum is much smaller. These findings agree with the anisotropy of the measured spectra of Ref. 12. In the case of PDA, Fig. 4 shows a similar behavior and the long-axis spectrum has an intense peak corresponding to the lowest singlet exciton. Here, however, additional structure is visible at higher photon energies. In particular, a resonance is observed around 8 eV in excellent agreement with the experimental resonance at 7.6 eV.[13] The intensity of the calculated resonance is quite small, though. For the perpendicular polarization, a number of low-intensity resonances are observed. The exciton effect is seen to produce a complete rearrangement of the spectra.

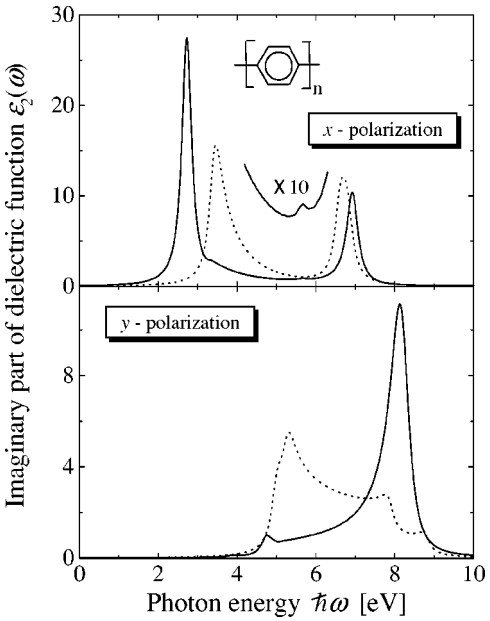

FIG. 5. Same as Fig. 3 but for poly-*para*-phenylene (PPP).

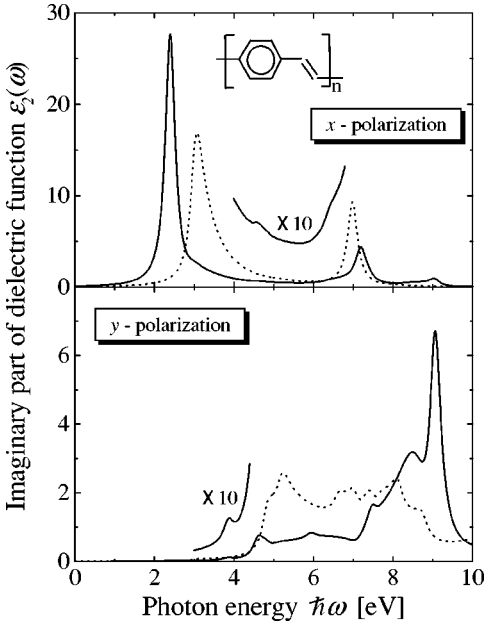

FIG. 6. Same as Fig. 3 but for polyphenylenevinylene (PPV). Notice the weak resonances at 4.6 and 3.8 eV in the magnified curves.

Turning now to the technologically more relevant polymers PPP and PPV, we find that exciton effects have a similarly dramatic influence on the optical spectra. For the long-axis absorption of PPP, the free-carrier calculation neglecting excitons predicts two resonances at 3.4 and 6.7 eV, cf. the dotted curve in the upper panel of Fig. 5. When excitons are included, these resonances shift to roughly 2.7 and 6.9 eV and a weak resonance appears around 5.7 eV. In addition, the excitonic spectrum for the perpendicular polarization has a relatively intense peak close to 4.8 eV while the free-carrier

peak is at 5.3 eV. To our knowledge, no experimental optical spectra for aligned ladder-type PPP have been published. Hence, we compare our calculation to measured spectra from thin films with random orientation of the polymer chains.[14] Apart from the fundamental resonance at 2.7 eV, to which the present calculation was adjusted, a second absorption band emerges at roughly 4.3 eV. This is in reasonable agreement with the calculated onset of absorption for the perpendicular polarization of 4.8 eV when exciton effects are taken into account.

The case of PPV is particularly interesting. Apart from excellent experimental data, a range of high quality calculations has been published. Experimentally, four peaks below 6 eV are detected for MEH-PPV: 2.4–2.5 eV, 3.6–3.7 eV, 4.7 eV, and 5.9–6.0 eV.[15,29] The first, second, and last of these are polarized along the long axis while the third at 4.7 eV is polarized off-axis with both short- and long-axis contributions. From the calculated spectra shown in Fig. 6, we find resonances at 2.4, 4.6, and 7.2 eV with long-axis polarization and at 3.8, 4.6, and 6.0 eV with short-axis polarization. In addition, a number of higher resonances are noticed. Thus, the predicted long-axis polarization of the lowest peak as well as the off-axis polarization of the peak at 4.6 eV is in clear agreement with experiments. The origin of the structure at 3.6–3.7 eV has been debated in the literature, and explanations based on broken charge-conjugation symmetry due to side-groups[37] or a finite-size effect resulting from chains with relatively few monomers[38] have been offered. The fact that the present calculation based on periodic boundary conditions predicts a resonance around 3.8 eV might point against explanations based on finite-size effects. However, the calculated resonance has the wrong polarization and therefore the present model obviously cannot provide the full explanation for this resonance.

As mentioned earlier, varying the transverse screening ε_y amounts to simulating polymer chains in different environments. The influence of the environment may be responsible for part of the discrepancy between the different experimental values for the exciton binding energies listed in Table II although different experimental techniques are probably the main reason. In order to give a quantitative measure of the influence of the environment, we have performed simulations of PPV using different values of ε_y in the range from $\varepsilon_y=2$ to $\varepsilon_y=4$, while keeping all other parameters fixed. The range from 2 to 4 should cover most solvents as well as polymer films with varying density. As expected, the spectra in Fig. 7 show that the exciton resonances shift to higher energy when screening is increased. In addition, the results in the inset show that the singlet binding energy changes from 0.41 eV at $\varepsilon_y=4$ to 1.04 eV at $\varepsilon_y=2$ whereas the triplet binding energy ranges between 0.86 and 1.69 eV. The overall shape of the spectra changes slightly in this screening range and the relative weight of the two polarizations is roughly constant. It is seen from the spectra, however, that the lowest singlet exciton around 2–3 eV tends to split off from the remaining absorption continuum when the binding energy is sufficiently high. It must be stressed, though, that the precise location of the resonances will depend also on the quasiparticle correction (scissors operator shift), which, in turn, is likely to depend on ε_y as well. The calculated binding energies are not affected by this uncertainty, however. From the results in Fig. 7, it is found that a singlet binding energy of 0.9 eV is obtained around $\varepsilon_y=2.3$. A binding energy of this magnitude was found for isolated PPV chains in Ref. 7 using full DFT and self-consistent screening. Thus, the value $\varepsilon_y=2.3$ can be used as an estimate of the transverse self-screening in conjugated polymers, i.e., the screening due to charges on the polymer chain itself rather than the surroundings.

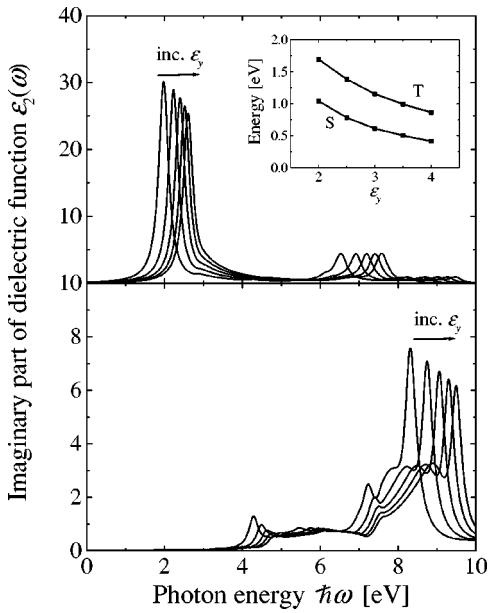

FIG. 7. x-polarized (upper panel) and y-polarized (lower panel) absorption spectra for PPV using values of ε_y ranging from $\varepsilon_y=2$ to $\varepsilon_y=4$ in steps of 0.5. Increasing ε_y leads to a blueshift of the exciton resonances. The inset illustrates the ε_y dependence of singlet (S) and triplet (T) exciton binding energies.

V. SUMMARY AND CONCLUSIONS

The density-functional-based formulation of the tight-binding method (DF-TB) has been applied to conjugated polymers. The relaxed geometry and electronic band-structure of four important materials (*trans*-polyacetylene, polydiacetylene, poly-*para*-phenylene, and polyphenylenevinylene) have been obtained from this non-self-consistent method. Exciton effects are subsequently incorporated via an expansion of the Bethe–Salpeter equation in the double basis formed by the tight-binding band states. A detailed discussion of the implementation of anisotropic screening has been included for this purpose. The theory has been applied to singlet as well as triplet excitons and, generally, rather close agreement with measurements has been found. Importantly, the UV/visible optical spectra calculated from the singlet excitons reproduce several features of the experimental spectra for the four materials including position and polarization of many resonances. We conclude that the DF-TB

DF-TB+Bethe–Salpeter approach provides a reliable and computationally efficient alternative to more sophisticated methods. Hence, application to structures, which are otherwise prohibitively complex, can be envisioned.

ACKNOWLEDGMENT

Financial support from the Danish Technical Research Council STVF is gratefully acknowledged.

[1] W. Hanke and L. J. Sham, Phys. Rev. B **21**, 4656 (1980).
[2] L. X. Benedict and E. L. Shirley, Phys. Rev. B **59**, 5441 (1999).
[3] M. Rohlfing and S. G. Louie, Phys. Rev. B **62**, 4927 (2000).
[4] P. Gomes da Costa and E. M. Conwell, Phys. Rev. B **48**, 1993 (1993).
[5] T. G. Pedersen, P. M. Johansen, and H. C. Pedersen, Phys. Rev. B **61**, 10504 (2000).
[6] T. G. Pedersen, Phys. Rev. B **67**, 073401 (2003).
[7] M. Rohlfing and S. G. Louie, Phys. Rev. Lett. **82**, 1959 (1999).
[8] J.-W. van der Horst, P. A. Bobbert, M. A. J. Michels, and H. Bässler, J. Chem. Phys. **114**, 6950 (2001).
[9] A. Ruini, M. J. Caldas, G. Bussi, and E. Molinari, Phys. Rev. Lett. **88**, 206403 (2002).
[10] T. G. Pedersen and T. B. Lynge, Comput. Mater. Sci. **27**, 123 (2003).
[11] D. Porezag, Th. Frauenheim, Th. Köhler, G. Seifert, and R. Kaschner, Phys. Rev. B **51**, 12947 (1995).
[12] G. Leising, Phys. Rev. B **38**, 10313 (1988).
[13] Y. Tokura, T. Mitani, and T. Koda, Chem. Phys. Lett. **75**, 324 (1980).
[14] M. G. Harrison, S. Möller, G. Weiser, G. Urbasch, R. F. Mahrt, H. Bässler, and U. Scherf, Phys. Rev. B **60**, 8650 (1999).
[15] E. K. Miller, D. Yoshida, C. Y. Yang, and A. J. Heeger, Phys. Rev. B **59**, 4661 (1998).
[16] Th. Frauenheim, F. Weich, Th. Köhler, S. Uhlmann, D. Porezag, and G. Seifert, Phys. Rev. B **52**, 11492 (1995).
[17] Th. Frauenheim, G. Seifert, M. Elstner, Z. Hajnal, G. Jungnickel, D. Porezag, S. Suhai, and R. Scholtz, Phys. Status Solidi B **217**, 41 (2000).
[18] G. Seifert, H. Terrones, M. Terrones, G. Jungnickel, and Th. Frauenheim, Phys. Rev. Lett. **85**, 146 (2000).
[19] G. Seifert, Th. Köhler, H. M. Urbassek, E. Hernández, and Th. Fraienheim, Phys. Rev. B **63**, 193409 (2001).
[20] T. G. Pedersen, K. Pedersen, P. K. Kristensen, J. Rafaelsen, N. skivesen, Z. Li, and S. V. Hoffmann, Surf. Sci. **516**, 127 (2002).
[21] S. Abe, J. Yu, and W. P. Su, Phys. Rev. B **45**, 8264 (1992).
[22] S. Abe, M. Schreiber, W. P. Su, and J. Yu, Phys. Rev. B **45**, 9432 (1992).
[23] S. Kivelson, W.-P. Su, J. R. Schrieffer, and A. J. Heeger, Phys. Rev. Lett. **58**, 1899 (1987).
[24] J.-W. van der Horst, P. A. Bobbert, M. A. J. Michels, G. Brocks, and P. J. Kelly, Phys. Rev. Lett. **83**, 4413 (1999).
[25] L. D. Landau and E. M. Lifshitz, *Electrodynamics of Continuous Media* (Pergamon, Oxford, 1969).
[26] L. X. Benedict, Phys. Rev. B **66**, 193105 (2002).
[27] D. Comoretto, R. Tubino, G. Dellepiane, G. F. Musso, A. Borghesi, A. Piaggi, and G. Lanzani, Phys. Rev. B **41**, 3534 (1990).
[28] T. G. Pedersen, K. Pedersen, and T. B. Kristensen, *ibid.* **63**, 201101 (2001).
[29] M. Liess, S. Jeglinski, Z. V. Vardeny, M. Ozaki, K. Yoshino, Y. Ding, and T. Barton, Phys. Rev. B **56**, 15712 (1997).
[30] A. Horvath, G. Weiser, C. Lapersonne-Meyer, M. Schott, and S. Spagnoli, Phys. Rev. B **53**, 13507 (1996).
[31] L. Robins, J. Orenstein, and R. Superfine, Phys. Rev. Lett. **56**, 1850 (1986).
[32] G. Meinhardt, A. Horvath, G. Weiser, and G. Leising, Synth. Met. **84**, 669 (1997).
[33] S. F. Alvarado, S. Barth, H. Bässler, U. Scherf, J.-W. van der Horst, P. A. Bobbert, and M. A. J. Michels, Adv. Funct. Mater. **12**, 117 (2002).
[34] Y. V. Romanovskii, A. Gerhard, B. Schweitzer, U. Scherf, R. I. Personov, and H. Bässler, Phys. Rev. Lett. **84**, 1027 (2000).
[35] J. M. Leng, S. Jeglinski, X. Wei, R. E. Benner, Z. V. Vardeny, F. Guo, and S. Mazumdar, Phys. Rev. Lett. **72**, 156 (1994).
[36] I. H. Campbell, T. W. Hagler, D. L. Smith, and J. P. Ferraris, Phys. Rev. Lett. **76**, 1900 (1996).
[37] Y. N. Gartstein, M. J. Rice, and E. M. Conwell, Synth. Met. **78**, 183 (1996).
[38] M. Chandross, S. Mazumdar, M. Liess, P. A. Lane, Z. V. Vardeny, M. Hamaguchi, and K. Yoshino, Phys. Rev. B **55**, 1486 (1997).